Introduction of a Fifth Carboxylate Ligand Heightens the Affinity of the Oncomodulin CD and EF Sites for Ca^{2+}†

Michael T. Henzl,* Raymond C. Hapak, and Emily A. Goodpasture

Department of Biochemistry, University of Missouri, Columbia, Missouri 65211

Received September 13, 1995; Revised Manuscript Received February 21, 1996⊗

ABSTRACT: The acid-pair hypothesis, proposed by Reid and Hodges [(1980) *J. Theor. Biol. 84*, 401−444], suggests that the affinity of an EF-hand motif for Ca^{2+} will be maximal with four acidic ligands, paired along the $+x,-x$ and $+z,-z$ axes. Addition of a fifth anionic ligand is predicted to reduce Ca^{2+}-binding affinity, as a consequence of increased electrostatic repulsion. Interestingly, for oncomodulin, we observe that introduction of a fifth carboxylate residue at the $+z$ position in the CD coordination sphere or at the $-x$ position in the EF coordination sphere significantly increases the affinity of those sites for Ca^{2+}. The variants resulting from replacement of serine-55 by aspartate (S55D), glycine-98 by aspartate (G98D), and the combined mutations (55/98) have been examined in Ca^{2+}- and Mg^{2+}-binding studies, titration calorimetry, and differential scanning calorimetry. The K_{Ca} for the CD site is reduced from 800 to 67 nM by the S55D mutation, while K_{Ca} for the EF site is reduced from 45 to 4 nM by the G98D mutation. Both mutations destabilize the apo form of the protein and increase the thermal stability on the Ca^{2+}-bound state. Interestingly, the S55D mutation also increases the affinity of the oncomodulin CD site for Mg^{2+}, decreasing the dissociation constant from >1 mM to approximately 30 μM. This increase in affinity is reflected in a substantially increased thermal stability of the Mg^{2+}-bound form of the protein. In 0.15 M NaCl, 0.025 M Hepes (pH 7.4), and 0.01 M Mg^{2+}, the wild-type protein denatures at 68.5 °C. By contrast, under identical conditions, the S55D mutation denatures at 79.0 °C. The increased metal ion-binding affinity displayed by the variant proteins may result in part from preferential destabilization of the apo-protein by the additional carboxylate.

The "EF-hand" domain is emblematic for the calmodulin superfamily (Kretsinger, 1980, 1987). This distinctive metal ion-binding motif consists of a 12-residue binding loop flanked by short helical segments. The ligands are positioned at the approximate vertices of an octahedron and are designated by the axes of a Cartesian coordinate system. Strictly speaking, however, the ligand geometry about the bound Ca^{2+} is pentagonal bipyramidal, since the $-z$ carboxylate is coordinated in a bidentate manner [e.g., Strynadka and James (1989)]. Despite their overall structural similarity, individual EF-hand domains exhibit substantial variation in their ion-binding properties. The observed dissociation constants for Ca^{2+}, for example, span 4 orders of magnitude, from $\approx 10^{-9}$ to 10^{-5} M (Seamon & Kretsinger, 1983).

Despite intense scrutiny of intact proteins and peptide model systems, the structural principles that govern ion-binding affinity in the EF-hand proteins remain incompletely understood [reviewed in Falke *et al.* (1994)]. On the basis of studies with peptide analogs of troponin C and calmodulin ion-binding domains, Reid and Hodges proposed the "acid-pair hypothesis" (Reid & Hodges, 1980). According to their hypothesis, the Ca^{2+} affinity of an EF-hand domain reflects an electrostatic compromise in which the penchant of the divalent cation for anionic (i.e., carboxylate) ligands is counterbalanced by the attendant interligand repulsion. A substantial body of data [e.g., Reid (1987, 1990) and Procyshyn and Reid (1994a,b)] suggests that Ca^{2+} affinity is maximized in a four-carboxylate site in which the carboxylates are paired on the $+x,-x$ and $+z,-z$ axes. In model systems, addition of a fifth carboxylate has been shown to reduce affinity, presumably due to uncompensated interligand repulsion [e.g., Marsden *et al.* (1988)].

The mammalian β-parvalbumin oncomodulin (MacManus & Whitfield, 1983) offers an attractive system for investigating determinants of ion-binding affinity in EF-hand proteins. Parvalbumins (Wnuk *et al.*, 1982; Heizmann, 1984; Gerday, 1988) contain two functional metal ion-binding sites, the CD[1] and EF sites, and the nonfunctional vestiges of a third (the AB domain). The CD site binding loop spans residues 51−62, in the approximate center of the primary structure, while the EF binding loop is located near the C-terminus, spanning residues 90−101 (for reference, the sequence of oncomodulin is displayed in Figure 1). The arrangement and identity of the ligands are quite typical of calmodulin superfamily members. The proximal ligands to the bound ion in the oncomodulin CD site are identical to those in site 2 of skeletal troponin C; similarly, the proximal ligands in the

† This work was supported by NSF Award MCB92−96171 (to M. T. H.). Portions of this work were presented at the Ninth International Symposium on Calcium-Binding Proteins and Calcium Function in Health and Disease in Airlie, VA, April 29 to May 3, 1995, and the 50th Calorimetry Conference in Gaithersburg, MD, July 23−28, 1995.

* To whom correspondence should be addressed.

⊗ Abstract published in *Advance ACS Abstracts,* April 15, 1996.

[1] Abbreviations: CD site, parvalbumin metal ion-binding site flanked by the C and D helical segments; EF site, parvalbumin metal ion-binding site flanked by the E and F helical segments; EDTA, ethylenediaminetetraacetic acid; Hepes, 4-(2-hydroxyethyl)-1-piperazineethanesulfonic acid; Tris, tris(hydroxymethyl)aminomethane; PV, parvalbumin; rOM, recombinant oncomodulin; wt, wild-type; S55D, OM variant resulting from replacement of serine-55 by aspartate; G98D, OM variant resulting from replacement of glycine-98 by aspartate; 55/98, OM variant resulting from the combined 55/98 mutations; DSC, differential scanning calorimetry.

S0006-2960(95)02184-2 CCC: $12.00

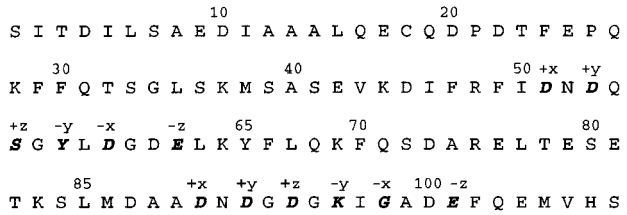

FIGURE 1: Amino acid sequence of rat oncomodulin. Coordinating residues are shown in italicized boldface type. Ligation occurs via side chain oxygen atoms, with several exceptions. Y57 and K96 coordinate via the main chain carbonyl oxygen; D59 coordinates via an intervening water molecule, and a water molecule serves as the ligand at residue 98 (Ahmed *et al*., 1990, 1993).

EF site are identical to those found in site 1 of calmodulin. As in other EF-hand proteins, the CD and EF sites are connected by a short antiparallel β-sheet involving residues 57−58 and 96−97, providing a potential mechanism for transmission of cooperative effects. However, the extent of cooperativity in the parvalbumins appears to be isoform-dependent. Although the whiting parvabumin binds Ca^{2+} in a positively cooperative manner (White, 1988), the majority of parvalbumin isoforms examined to date exhibit noncooperative binding. Significantly, the parvalbumin tertiary structure is distinguished from other calmodulin family members by the presence of the AB domain, which packs tightly against the hydrophobic aspect of the CD/EF domain.

Typically, the parvalbumin CD and EF sites are "Ca^{2+}/Mg^{2+}" sites, exhibiting high affinity for Ca^{2+} ($K_d < 10^{-7}$ M) and substantial affinity for Mg^{2+} ($K_d < 10^{-4}$ M) as well. Despite a high degree of sequence homology to other PV isoforms, oncomodulin displays markedly attenuated affinity for Ca^{2+} and Mg^{2+}. In fact, with $K_{Ca} \approx 1$ μM and $K_{Mg} > 1$ mM, the CD site of OM qualifies as a "Ca^{2+}-specific" site (Hapak *et al.*, 1989; Cox *et al.*, 1990). For several years, we and others have been attempting to identify factors responsible for the decrease in ion-binding affinity (Hapak *et al.*, 1989; Golden *et al.*, 1990; Palmisano *et al.*, 1990; Treviño *et al.*, 1991).

Initially, we prepared the S55D variant in order to examine certain nuances associated with the Eu^{3+} $^7F_0 \rightarrow {}^5D_0$ excitation spectra of Eu^{3+}-bound parvalbumins (Henzl *et al.*, 1992; Kauffman *et al.*, 1995). In due course, we measured the Ca^{2+} dissociation constants for the variant protein, expecting to observe a reduction in affinity. Unexpectedly, we discovered that the affinity of the CD site was substantially increased. Excited by this finding, we turned our attention to G98D and, subsequently, the double variant S55D/G98D (55/98). We have now examined these three proteins by flow dialysis, titration calorimetry, and differential scanning calorimetry. The results of these studies offer insight into mechanisms underlying alterations in ion-binding affinity among the EF-hand proteins.

MATERIALS AND METHODS

Oncomodulin (OM) and site-specific variants thereof were produced and isolated by methods described previously (Hapak *et al.*, 1989). The purified proteins were passed over EDTA−agarose at pH 7.4 to remove bound Ca^{2+} (Haner *et al.*, 1984). The residual Ca^{2+} content, estimated by flame atomic absorption spectroscopy, was ≤ 0.05 molar equiv in all cases. Buffers used for metal ion analyses were similarly cleansed of divalent metal ions by passage over the chelating matrix.

Preliminary estimates of protein concentration were obtained by titrating 2.0 mL samples of the protein of interest ($\approx$20 μM) with 1.0 mM Tb^{3+}, monitoring the pronounced increase in sensitized luminescence ($\lambda_{ex} = 280$ nm, $\lambda_{em} = 545$ nm) that accompanies binding of the lanthanide ion to the protein (see below). The apparent end point in the titration corresponds to addition of 2.0 molar equiv of the ion.

Titration Calorimetry. Calorimetric titrations on rOM, S55D, G98D, and 55/98 proteins were performed at 25 °C in an isothermal titration calorimeter from Calorimetric Sciences Corp. (Provo, UT) interfaced with a desktop personal computer. Following equilibration, 4.0 μL additions of titrant were made automatically to the 1.00 mL sample at 200 s intervals from a 100 μL Hamilton syringe driven by a precision stepper motor. In all cases, the sample buffer consisted of 0.15 M NaCl and 0.025 M Hepes-NaOH (pH 7.4). The reference cell contained 1.00 mL of water.

The heat fluxes that accompanied binding were collected, stored, and integrated using software supplied with the instrument. Prior to curve fitting, the data were corrected for the heat of titrant dilution by subtracting the results of a blank titration. Enthalpies of binding were extracted from the data using the BindWorks software package (v. 1.0b, Applied Thermodynamics). The analyses utilized the following model describing two classes of independent binding sites (Freire *et al.*, 1990):

$$Q = Q_1 + Q_2 = (\Delta H_1[L_{B,1}] + \Delta H_2[L_{B,2}])V \quad (1)$$

$$Q = V[M]\left(\frac{n_1 \Delta H_1 K_1[L]}{1 + K_1[L]} + \frac{n_2 \Delta H_2 K_2[L]}{1 + K_2[L]}\right) \quad (2)$$

$$[L_{B,1}] = [M]\left(\frac{n_1 \Delta H_1 K_1[L]}{1 + K_1[L]}\right); [L_{B,2}] = [M]\left(\frac{n_2 \Delta H_2 K_2[L]}{1 + K_2[L]}\right) \quad (3)$$

$$[L] = [L_T] - [M]\left[\frac{n_1 K_1[L](1 + K_2[L]) + n_2 K_2[L](1 + K_1[L])}{(1 + K_1[L])(1 + K_2[L])}\right] \quad (4)$$

The subscripts 1 and 2 denote the two classes of binding sites. n_1 and n_2 are the number of sites in each class. ΔH and K represent the molar enthalpy of ligand binding and the ligand association constant, respectively. [L] is the free ligand concentration. $[L_{B,1}]$ and $[L_{B,2}]$ represent the concentrations of ligand bound at each of the two classes of sites. [M] is the total protein concentration. V is the sample volume. Q, Q_1, and Q_2 represent the total heat of binding and the heats associated with the binding events at each class of sites.

For the least-squares analyses, the binding constants were fixed at the values obtained by direct binding studies. R^2, as defined below, exceeded 0.99 in all cases.

$$R^2 = \frac{|\sum_{i=1}^{n} Y_{\mathrm{obs}_i}{}^2 - \sum_{i=1}^{n} (Y_{\mathrm{obs}_i} - Y_{\mathrm{cal}_i})^2|}{\sum_{i=1}^{n} Y_{\mathrm{obs}_i}{}^2} \quad (5)$$

Y_{obs} and Y_{cal} represent the observed and calculated values, respectively, for a particular data point.

The heat of protonation of Tris base was used to calibrate the titration calorimeter. At 25 °C, this quantity is calculated to be −11.36 kcal/mol, from the relationship reported by Christensen *et al.* (1976); $H_{prot} = -11.880 + 0.0244t - (1.418 \times 10^{-4})t^2$, where t is the temperature in degrees Celsius. The performance of the instrument was evaluated by titrating a sample of the crown ether, 18-crown-6, with Ba^{2+}. The enthalpy and dissociation constant for complexation of Ba^{2+} by this crown ether are −7.47 ± 0.095 kcal/mol and (1.738 ± 0.39) × 10^{-4} M, respectively (Briggner & Wadsö, 1991). Excellent agreement with the literature values was obtained.

Scanning calorimetry was performed in a differential scanning calorimeter from Calorimetry Sciences Corp. The samples (0.5000 ± 0.0002 g) were contained in removable stainless steel ampules. The four-cell design of the instrument permits three samples to be examined during a scan. For the experiments discussed below, we included apo, Mg^{2+}-bound, and Ca^{2+}-bound samples of a given variant. A solid metal ampule, having a heat capacity equal to 0.500 g of water, served as the reference cell.

Prior to analysis, protein samples were dialyzed against a 100-fold excess of the appropriate buffer. The apo samples were dialyzed against 0.15 M NaCl, 0.025 M Hepes-NaOH, and 5 mM EDTA (pH 7.4); the Ca^{2+}-bound samples were dialyzed against 0.15 M NaCl, 0.025 M Hepes-NaOH, and 5.0 mM Ca^{2+} (pH 7.4), and the Mg^{2+}-bound samples were dialyzed against 0.15 M NaCl, 0.025 M Hepes-NaOH, 20.0 mM Mg^{2+}, and 1.0 mM EGTA (pH 7.4). The identical dialysis buffer was employed for each of the four proteins examined to eliminate variations arising from minor differences in buffer composition. Baseline scans were subsequently performed on the dialysis buffer alone. All of the data presented were collected at a scan rate of 60 °C/h. Scans collected on wild-type rOM and the S55D variant exhibited the same line width and excess heat capacity at scan rates of 30 and 60 °C/h. These findings indicate that equilibrium was maintained in the samples at the higher scan rate and also suggest that the thermal denaturation is thermodynamically reversible.

The fusion of water was used to calibrate both the temperature and response of the instrument. Ampoules containing 0.100 g of deionized water were placed in the instrument and cooled to −20 °C. After 1 h, the calorimeter temperature was raised to −5 °C, and a scan was performed to +5 °C at a rate of 2 °C/h. The area under the peak corresponds to the heat of fusion of water (79.88 cal/g), while the peak maximum represents the melting temperature of water (0 °C).

Data were analyzed with software supplied with the instrument. Raw voltage data were converted to heat capacities, and a baseline scan (buffer alone) was subtracted from the protein data. Residual curvature was removed by fitting a fourth-order polynomial to the pre- and post-transition regions of the baseline and then subtracting the polynomial from the corrected protein scan. The calorimetric enthalpy (ΔH_{cal}) was determined by integrating the area under the peak. The van't Hoff, or effective, enthalpy (ΔH_{vH}) was calculated by the following equation:

$$\Delta H_{vH} = 4RT_d{}^2 \frac{\Delta C_{p,max}}{Q} \quad (6)$$

in which R is the gas constant, T_d is the temperature at the peak of the thermal transition, $\Delta C_{p,max}$ is the excess heat capacity at T_d, and Q is the area under the transition peak [e.g., Sturtevant (1987)].

NMR Spectroscopy. One-dimensional ^{1}H NMR spectra were acquired at 37 °C on a Bruker AMX500 spectrometer, employing a transmitter frequency of 500 MHz, an 8.0 μs pulse length, and a 2.0 s acquisition period. The water signal was suppressed by presaturation for 1.5 s. Each spectrum represents the sum of 80 transients. Chemical shifts are reported relative to TSP in D_2O. Samples (0.6 mL) of the apo-proteins, at concentrations between 2.6 and 3.0 mM, were prepared in 0.15 M NaCl (pH 7.4) and 10% (v/v) D_2O and placed in 5 mm inside diameter (i.d.) NMR tubes. Aliquots of Ca^{2+} or Mg^{2+}, prepared in the identical buffer, were added to the samples with a 50 μL Hamilton syringe equipped with a 30 cm needle. After each addition, the samples were mixed with a 1.0 mL Hamilton similarly equipped with a 30 cm needle. The spectra are uncorrected for dilution, which was less than 10% in each experiment.

Least-squares analyses of metal ion-binding data were performed with the Scientist program from MicroMath, Inc. (Salt Lake City, UT). Scientist permits the model to be entered as a system of equations harboring one or more implicit variables. Analyses were performed on a desktop computer equipped with an 80486 processor and a math coprocessor. In every case, the R^2 value (defined above) exceeded 0.99. The reported parameter values represent the mean of several determinations and are reported along with the greatest deviation from the mean value.

Ca^{2+}-binding affinities for each of the four proteins discussed in this paper were measured by flow dialysis (Colowick & Womack, 1967; Hapak *et al.*, 1989; Palmisano *et al.*, 1990). The binding data obtained for each of these proteins can be satisfactorily accommodated by an independent two-site model:

$$r = \frac{[Ca^{2+}]}{k_1 + [Ca^{2+}]} + \frac{[Ca^{2+}]}{k_2 + [Ca^{2+}]} \quad (7)$$

where r is the average number of moles of Ca^{2+} bound per mole of protein and k_1 and k_2 are the apparent dissociation constants for the two binding sites.

Mg^{2+} dissociation constants were estimated from $^{45}Ca^{2+}$ flow dialysis data gathered in the presence of fixed levels of Mg^{2+} ion. When the competing Mg^{2+} ion is present in large excess over the protein, the free Mg^{2+} concentration is essentially throughout the course of the titration. Under these conditions, the apparent Ca^{2+} dissociation constant (K_{Ca}') is related to the true value (K_{Ca}) by the following expression:

$$K_{Ca}' = K_{Ca}\left(1 + \frac{[Mg^{2+}]}{K_{Mg}}\right) \quad (8)$$

The slope of the line relating K_{Ca}' and $[Mg^{2+}]$ is equal to K_{Ca}/K_{Mg}. Since the protein concentration employed in these studies was 100 μM, the assumption that the free Mg^{2+} level is essentially constant throughout the titration was valid at total Mg^{2+} levels exceeding 2.0 mM.

At lower concentrations of Mg^{2+}, the free Mg^{2+} concentration (M) varies throughout the course of the titration, causing likewise variation in the apparent Ca^{2+} dissociation constants, K1A and K2A. To extract the Mg^{2+} dissociation constants (K1M and K2M) from data gathered under these conditions, we employed the following model within the Scientist program. The independent variable is the free Ca^{2+} concentration (C), determined from analysis of the flow dialysis data. The dependent variable is R, the average number of moles of Ca^{2+} bound per mole of protein. Although M is not constant during the experiment, the true and apparent Ca^{2+} dissociation constants are nevertheless related by eq 2. At each point in the titration, the average number of moles of Ca^{2+} bound per mole of protein is given by the relationship

$$R = \frac{C}{\mathrm{K1A} + C} + \frac{C}{\mathrm{K2A} + C} \quad (9)$$

where

$$\mathrm{K1A} = \mathrm{K1}\left(1 + \frac{M}{\mathrm{K1M}}\right) \text{ and } \mathrm{K2A} = \mathrm{K2}\left(1 + \frac{M}{\mathrm{K2M}}\right) \quad (10)$$

The value of M at each point in the titration is not known explicitly but can be derived implicitly, subject to the constraint that the total Mg^{2+} concentration (MT) must equal the sum of the free and the bound concentrations:

$$\mathrm{MT} = M + \frac{MP}{\mathrm{K1M} + \mathrm{M}} + \frac{MP}{\mathrm{K2M} + M} \quad (11)$$

where P is the protein concentration. The Scientist program, supplied with the true Ca^{2+} dissociation constants (K1 and K2, determined in the absence of Mg^{2+}) and the protein concentration, varies K1M and K2M so as to minimize the sum of the squares error, $(R_{obs} - R_{calc})^2$.

The interaction between Mg^{2+} and oncomodulin was also examined by equilibrium dialysis, in dialysis blocks of standard design having nominal 1.0 mL sample capacities. Lateral transfer of material between wells was prevented by the use of hand-cut Parafilm gaskets. The dialysis blocks and parafilm gaskets were soaked in 3% HNO_3 and thoroughly rinsed with deionized water prior to assembly. Dialysis membrane (Spectrapor 1, molecular weight cutoff of 6000−8000) was treated with hot (70 °C) 1% sodium carbonate, thoroughly rinsed in deionized water, and stored in 20% ethanol. Immediately prior to use, the tubing was cut along one edge, opened flat, and then soaked for 30 min in 3% HNO_3, after which it was thoroughly rinsed in deionized water.

The 0.60 mL protein samples [600 μM in 0.15 M NaCl and 0.025 M Hepes-NaOH (pH 7.4)] were added through the sample ports to the protein chambers by syringe. Buffer and Mg^{2+} (600 μL total) were added to the opposing chambers. After the samples were in place, the edges of the blocks were sealed with Parafilm to minimize evaporation, and the blocks were placed on a rocking platform in an incubator at 25 °C and allowed to equilibrate for 20−24 h. Mg^{2+} levels were measured by atomic absorption.

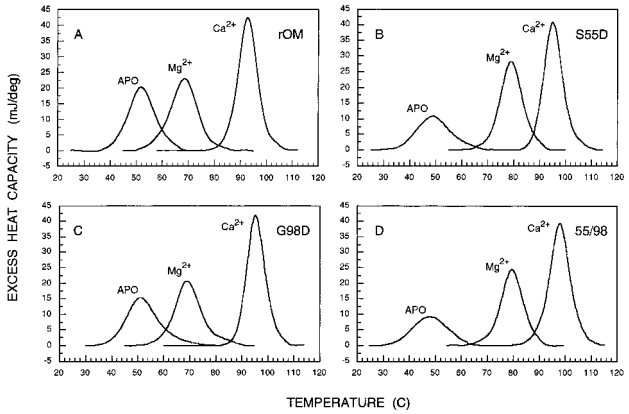

FIGURE 2: Conformational stabilities of rOM, S55D, G98D, and 55/98. Samples of the four proteins were analyzed by DSC as described in Materials and Methods, in 0.15 M NaCl and 0.015 M Hepes-NaOH (pH 7.4). The following concentrations were employed: rOM, 1.3 mM; S55D, 1.1 mM; G98D, 1.2 mM; and 55/98, 1.1 mM. The apo-protein samples contained 5 mM EDTA; the Ca^{2+}-bound samples contained 5.0 mM free Ca^{2+}, and the Mg^{2+}-bound protein samples contained 20 mM Mg^{2+} and 1.0 mM EGTA.

RESULTS

Differential Scanning Calorimetry. Since the impact of the S55D and G98D mutations on metal ion-binding affinity is closely related to the issue of conformational stability, we have examined the S55D, G98D, and 55/98 variants by differential scanning calorimetry in the absence and presence of Ca^{2+} and Mg^{2+}.

In 1978, Privalov and co-workers examined carp PV by DSC (Filimonov *et al.*, 1978). They observed that the apoprotein exhibits marginal stability at low ionic strengths, denaturing at 36 °C in 0.010 M sodium phosphate and 5 mM EDTA (pH 7.5). Addition of 1 M NaCl shifted the transition to 52 °C, indicating a large electrostatic contribution to the conformational free energy. This electrostatic component is a consequence of the substantial negative charge on the molecule at neutral pH. For oncomodulin, the net charge on the molecule at pH 7.4 is predicted to be −15 on the basis of the presence of 15 Asp, 9 Glu, 7 Lys, and 2 Arg residues (Gillen *et al.*, 1987). Thus, it is anticipated that electrostatic interactions will strongly influence the conformational stability of oncomodulin as well.

Representative DSC data for wild-type oncomodulin and the variant proteins are displayed in Figure 2, and the relevant DSC parameters are listed in Table 1. As shown in Figure 2A, the apo form of rOM denatures at 51.8 °C, comparable to the behavior observed by Privalov and colleagues with carp parvalbumin. Denaturation is apparently a two-state transition, as indicated by the near equality of the van't Hoff and calorimetric enthalpies. The conformational stability (ΔG_{conf}) of a protein at any temperature T can be estimated from its DSC behavior using the following equation:

$$\Delta G_{conf}(\mathrm{T}) = \Delta H_d(T_d - T)/T_d - \Delta C_p(T_d - T) + T\Delta C_p \ln(T_d/T) \quad (12)$$

where ΔC_p is the change in partial molar heat capacity upon

Table 1: Summary of DSC Data on rOM, S55D, G98D, and 55/98[a]

protein	apo-proteins					Ca^{2+}-bound proteins						Mg^{2+}-bound proteins				
	T_d	ΔT_d	ΔH_{cal}	$\Delta H_{cal}/\Delta H_{vH}$	ΔG_{conf}[b] (25 °C)	$\Delta\Delta G_{conf}$[c]	T_d	ΔT_d	ΔH_{cal}	$\Delta H_{cal}/\Delta H_{vH}$	ΔG_{conf}[b] (25 °C)	$\Delta\Delta G_{conf}$[c]	T_d	ΔT_d	ΔH_{cal}	$\Delta H_{cal}/\Delta H_{vH}$	$\Delta\Delta G_{conf}$[d]
rOM	51.8	–	66 ± 4	1.01	3.9 ± 0.4	–	92.8	–	108 ± 5	0.98	12.6 ± 1.0	–	68.5	–	88 ± 4	1.30	–
S55D	48.9	−2.9	51 ± 3	0.97	2.6 ± 0.3	−1.3	95.1	2.3	110 ± 5	1.02	13.1 ± 1.0	+0.5	79.0	10.5	93 ± 5	1.02	2.7
G98D	51.1	−0.7	58 ± 4	0.99	3.2 ± 0.3	−0.7	95.3	2.5	120 ± 6	1.01	15.0 ± 1.0	+2.4	69.0	0.5	91 ± 5	1.29	0.1
55/98	47.9	−3.9	49 ± 3	1.03	2.4 ± 0.3	−1.5	97.4	4.6	124 ± 6	1.02	15.9 ± 1.0	+3.3	79.4	10.9	91 ± 5	0.98	2.8

[a] All energies are expressed in kilocalories per mole. [b] Conformational free energy at 25 °C, calculated with eq 12, using the observed ΔH_{cal} values and the values of ΔC_p reported by Filimonov *et al.* (1978) for the apo- (1.33 kcal mol^{-1} K^{-1}) and Ca^{2+}-bound (1.10 kcal mol^{-1} K^{-1}) proteins. [c] Change in conformational free energy at 25 °C resulting from a given mutation. [d] Change in conformational free energy, calculated with eq 13.

denaturation and ΔH_{cal} is the enthalpy of denaturation at T_d, the temperature of denaturation [e.g., Privalov (1979)]. Employing the observed ΔH_{cal} value of 66 ± 4 kcal/mol and the ΔC_p value of 1.33 kcal mol^{-1} K^{-1} reported by Filimonov *et al.* for the apo form of carp parvalbumin, we calculate a conformational stability for apo-rOM at 25 °C of 3.9 ± 0.4 kcal/mol.

The apo forms of S55D, G98D, and 55/98 all exhibit reduced conformational stability. Replacement of serine-55 by aspartate shifts the transition temperature for the apo-protein downward to 48.9 °C ($\Delta T_d = -2.9$, Figure 2B) and reduces ΔH_{cal} to 51 ± 4 kcal/mol. Replacement of glycine-98 by aspartate causes somewhat smaller reductions in T_d and ΔH_{cal} (Figure 2C), to 51.1 °C and 58 ± 4 kcal/mol, respectively. Finally, combination of the S55D and G98D mutations shifts the melting temperature for the apo-protein downward by 3.9 °C to 47.9 °C (Figure 2D) and reduces ΔH_{cal} to 49 ± 4 kcal/mol. Substituting the observed values for T_d and ΔH_{cal} into eq 12, we calculate stabilities for S55D, G98D, and 55/98 at 25 °C of 2.6, 3.2, and 2.4 kcal/mol, respectively.

In contrast to the apo-proteins, Ca^{2+}-bound parvalbumins exhibit remarkable thermal stability. Filimonov *et al.* (1978), for example, observed that the addition of Ca^{2+} raised the transition temperature for carp PV to about 90 °C. rOM shows a comparable increase in stability in the Ca^{2+}-bound form. In the presence of 5.0 mM Ca^{2+}, the loss of native structure occurs at a temperature of 92.8 °C (Figure 2A). The observed ΔH_{cal} for Ca^{2+}-bound rOM is 108 ± 5 kcal/mol, comparable to the value reported for carp PV. The ratio of $\Delta H_{cal}/\Delta H_{vH}$ is nearly 1.0, indicating that the denaturation is two-state, with negligible population of intermediate states. The high Ca^{2+} concentration (≥5000 times the K_d for the weaker site) presumably maintains the protein in the fully ligated state until denaturation occurs [e.g., Brandts and Lin (1990) and Straume and Freire (1992)]. Substituting the observed values of T_d and ΔH_{cal} into eq 12, along with the ΔC_p value of 1.10 kcal mol^{-1} K^{-1} reported by Filimonov *et al.* (1978) for Ca^{2+}-bound carp PV, we estimate a conformational stability for Ca^{2+}-bound rOM at 25 °C of 12.6 ± 1.0 kcal/mol. Reduced electrostatic repulsion and the highly favorable free energy of Ca^{2+} binding are probably responsible for the increased stability of the Ca^{2+}-ligated form.

Whereas the S55D and G98D mutations destabilize the apo-protein, they increase the thermal stability of the Ca^{2+}-bound protein. The melting point for the Ca^{2+}-bound form of the protein is shifted upward to 95.1 °C ($\Delta T_d = 2.3$) by the S55D mutation (Figure 2B). The calculated stability at 25 °C is 13.1 ± 1.0 kcal/mol. The Ca^{2+}-bound form of G98D (Figure 2C) shows a nearly identical transition temperature of 95.3 °C ($\Delta T_d = 2.5$) and a slightly higher value of ΔH_{cal}. The predicted stability of G98D at 25 °C is 15.0 ± 1.0 kcal/mol. The 55/98 double variant (Figure 2D) displays still greater stability, denaturing at 97.4 °C ($\Delta T_d = 4.6$) with $\Delta H_{cal} = 124 \pm 5$ kcal/mol. The calculated stability at 25 °C is 15.9 ± 1.0 kcal/mol. The increases in conformational stability attendant to the S55D, G98D, and 55/98 mutations are 0.5, 2.4, and 3.3 kcal/mol, respectively.

In the presence of 20 mM Mg^{2+}, wild-type rOM denatures at 68.5 °C with an apparent enthalpy of denaturation of 88 ± 5 kcal/mol (Figure 2A). The ratio of $\Delta H_{cal}/\Delta H_{vH} = 1.3$, indicating that the denaturation is not a two-state transition.

Table 2: Summary of Metal Ion-Binding Properties[a]

		Ca^{2+} binding							Mg^{2+} binding		
protein	site	K_{Ca}[b] (nM)	$G_{Ca}{}^{o\prime}$[c]	H_{Ca}	$-T\Delta S_{Ca}$	ΔG_{Ca}[d]	ΔH_{Ca}[d]	$-T\Delta\Delta S_{Ca}$[d]	K_{Mg}[b] (μM)	$G_{Mg}{}^{o\prime}$[c]	ΔG_{Mg}[d]
rOM	CD	800 ± 30	-8.3	-3.43 ± 0.12	-4.9	–	–	–	1510 ± 180	-3.8	–
	EF	45 ± 5	-10.0	-4.06 ± 0.03	-5.9	–	–	–	260 ± 100	-4.9	–
	combined	–	-18.3	-7.5	-10.8	–	–	–	–	-8.7	–
G98D	CD	800 ± 40	-8.3	-3.42 ± 0.07	-4.9	0	0	0	3700 ± 400	-3.3	$+0.5$
	EF	4 ± 3	-11.4	-4.01 ± 0.03	-7.4	-1.4	$+0.1$	-1.5	130 ± 30	-5.3	-0.4
	combined	–	-19.7	-7.4	-12.3	-1.4	$+0.1$	-1.5	–	-8.6	$+0.1$
S55D	CD	67 ± 12	-9.7	-2.45 ± 0.15	-7.3	-1.4	$+1.0$	-2.4	29 ± 4	-6.2	-2.4
	EF	26 ± 5	-10.3	-6.73 ± 0.03	-3.6	-0.3	-2.6	$+2.3$	93 ± 10	-5.5	-0.6
	combined	–	-20.0	-9.1	-10.9	-1.7	-1.6	-0.1	–	-11.7	-3.0
55/98	CD	45 ± 15	-10.0	-3.87 ± 0.33	-6.1	-1.7	-0.5	-1.2	31 ± 3	-6.1	-2.3
	EF	4 ± 2	-11.4	-6.76 ± 0.23	-4.6	-1.4	-2.7	$+1.3$	165 ± 12	-5.1	-0.2
	combined	–	-21.4	-10.7	-10.7	-3.1	-3.2	$+0.1$	–	-11.2	-2.5

[a] All energies are expressed as kilocalories per mole. [b] K_{Ca} and K_{Mg} refer to the dissociation constants for Ca^{2+} and Mg^{2+} binding. [c] The standard free energy change for Ca^{2+} binding ($\Delta G_{Ca}{}^{o\prime}$) was calulated with the equation $\Delta G^{o\prime} = -(-RT \ln K_{Ca})$. [d] $\Delta\Delta G_{Ca}$ denotes the change in the free energy of binding caused by the mutation, relative to the wild-type protein. $\Delta\Delta H_{Ca}$ and $-T\Delta\Delta S_{Ca}$ denote the corresponding changes in the enthalpic and entropic contributions resulting from the mutation.

This is not unexpected, since the CD site of rOM would not be completely occupied by Mg^{2+}, even at a concentration of 20 mM (see below). In view of the decidedly non-two-state behavior and for want of a reliable value of ΔC_p for the Mg^{2+}-bound protein [not determined by Filimonov *et al.* (1978)], we have not calculated conformational stabilities for the Mg^{2+}-bound proteins.

The S55D mutation substantially increases the stability of OM in the presence of Mg^{2+}, shifting the melting temperature to 79.0 °C (Figure 2B). In contrast to S55D, the G98D mutation leaves T_d nearly unchanged (Figure 2C). As discussed below, the increase in Mg^{2+} affinity at the EF site is almost exactly offset by a decrease in affinity at the CD site. Consequently, the thermal stability of the Mg^{2+}-bound G98D variant closely resembles that for wild-type rOM. The behavior of the 55/98 variant resembles that observed for S55D, denaturing at 79.4 °C.

Although we cannot calculate the absolute conformational stabilities of the Mg^{2+}-bound proteins, we can nevertheless estimate the changes in stability $\Delta\Delta G_{conf}$ resulting from the S55D, G98D, and 55/98 mutations by means of eq 13:

$$\Delta\Delta G_{conf} = \Delta T_d \Delta H_{d,wt}/T_{d,wt} \qquad (13)$$

In this equation, ΔT_d is the shift in melting temperature due to the mutation of interest and $\Delta H_{d,wt}$ and $\Delta T_{d,wt}$ are the melting temperature and enthalpy of denaturation for the wild-type protein. This treatment, described by Bechtel and Schellman (1987), assumes only that the mutation under consideration qualifies as a minimal perturbation, i.e., that it causes a minor structural perturbation. Since the mutations under consideration here do not substantially alter the number of apolar hydrogen atoms per residue, the average number of H bonds per residue, or the conformational entropy per residue, this assumption is likely to be correct. Using eq 13, we calculate that the stabilities of the S55D and 55/98 variants, respectively, are 2.7 and 2.8 kcal/mol greater than that of the wild-type protein in the presence of 20 mM Mg^{2+}. The stability of the G98D variant is essentially unchanged.

Metal Ion-Binding Properties. The thermodynamic parameters describing the interactions between Ca^{2+} and Mg^{2+} and the oncomodulin variants have been determined from direct-binding experiments and titration calorimetry and are tabulated in Table 2. In the following paragraphs, we describe our findings, beginning with wild-type rOM. The

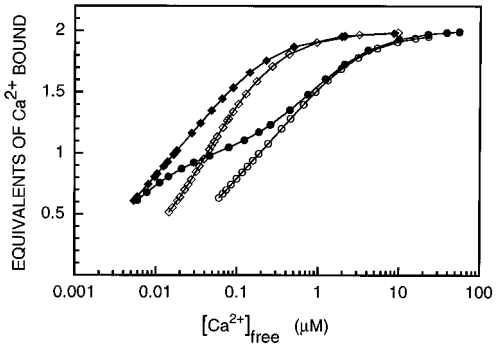

FIGURE 3: Titration of S55D, G98D, and 55/98 variants with Ca^{2+}. Samples (100 μM) of the proteins were examined by flow dialysis, either in the absence or in the presence of competing Mg^{2+}: wild-type rOM (○), G98D (●), S55D (◇), and 55/98 (◆).

CD and EF sites in this protein are decidedly nonequivalent. Lacking site-specific signals for the two sites, we have chosen to treat the protein as an independent two-site system. Our data are accomodated quite well by this minimal model. Moreover, it is not generally possible [e.g., Wyman and Gill (1990)] to assess cooperativity in systems harboring nonequivalent sites on the basis of direct binding studies alone. This does not mean, however, that cooperative effects are not operating. In fact, there are several instances in which the dissociation constant at one of the sites has been perturbed by the mutation at the remote site. We will mention these as they are encountered.

rOM. As initially reported by Hapak *et al.* (1989), wild-type oncomodulin displays apparent Ca^{2+} dissociation constants for the CD and EF sites of 800 ± 30 and 45 ± 5 nM, respectively. Comparable values were also reported by Cox *et al.* (1990). Representative data from our laboratory are presented in Figure 3 (○). The fit to this data obtained using eq 7 with $k_1 = 48$ nM and $k_2 = 820$ nM is indicated by the solid line through the points.

The enthalpy changes that accompany binding of Ca^{2+} and Mg^{2+} to oncomodulin were previously measured by Cox *et al.* (1990) using flow calorimetry. They reported that the heats of Ca^{2+} binding for the CD and EF sites, at pH 7.4 and 25 °C in 0.15 M NaCl and 0.025 M Hepes-NaOH, were essentially indistinguishable, approximately -4.5 kcal/mol. Calorimetry data for wild-type oncomodulin from this lab are presented in Figure 4. The individual heat fluxes that

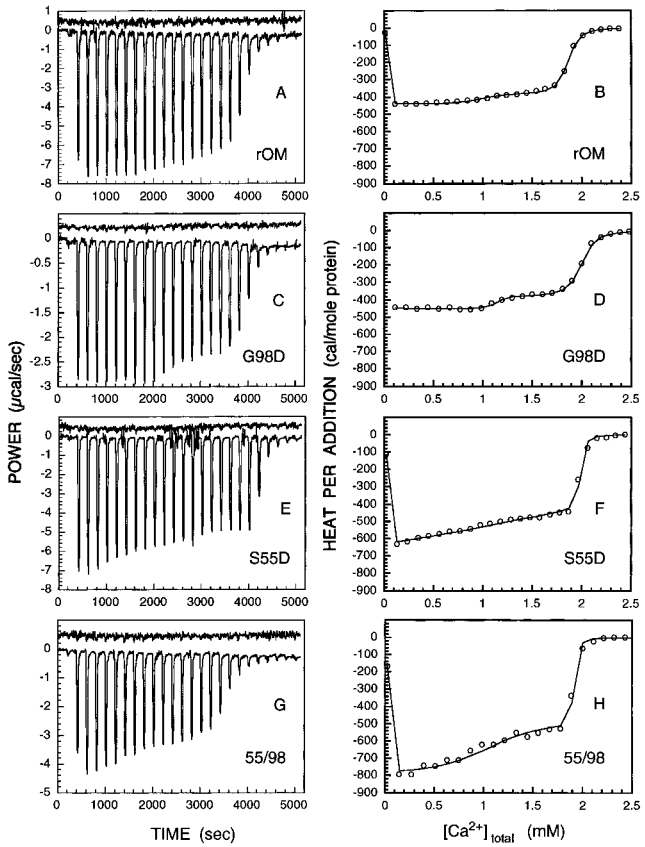

FIGURE 4: Calorimetric analysis of Ca^{2+} binding to rOM, S55D, G98D, and 55/98. Binding of Ca^{2+} to each of the four proteins was examined by titration calorimetry, as described in Materials and Methods. The individual heat effects that accompanied addition of Ca^{2+} are shown in the panels on the left. Data for the corresponding titration of buffer alone are shown for comparison, offset by +0.5 μcal/s for clarity. The integrated heat (○) evolved per addition is displayed as a function of total Ca^{2+} added in the right-hand panels. The solid line through the data represents the best least-squares fit to an independent two-site model, fixing the dissociation constants at the values determined by flow dialysis. The protein concentrations were as follows: rOM, 550 μM; S55D, 180 μM; G98D, 210 μM; and 55/98, 160 μM.

accompanied each addition of Ca^{2+} are displayed in panel A. The integrated heat evolved per addition, corrected for the heat of mixing, is plotted as a function of the total added Ca^{2+} in Figure 4B. The enthalpies of binding were estimated with the BindWorks software, utilizing the independent two-site model specified by eqs 1−4.

The best least-squares fit to the calorimetry data is indicated by the solid line in panel B. The optimal values for H_{EF} and H_{CD} were determined to be −4.07 and −3.49 kcal/mol. The average values, obtained from least-squares analysis of three experiments, were −4.06 ± 0.03 and −3.44 ± 0.05 kcal/mol. This result compares favorably with the previous estimates of Cox *et al.*, although it suggests that the Ca^{2+}-binding event at the CD site may be slightly less exothermic than the corresponding event at the EF site.

Whereas there seems to be some agreement with regard to the Ca^{2+}-binding properties of oncomodulin, the affinity of the protein for Mg^{2+} is more controversial. Hapak *et al.* (1989) previously reported Mg^{2+} dissociation constants of 0.16 and 3 mM for the EF and CD sites, on the basis of $^{45}Ca^{2+}$ flow dialysis measurements conducted in the presence of 1.0 mM Mg^{2+}. However, Cox *et al.* (1990) reported that Mg^{2+} binding was effectively confined to the EF site, since

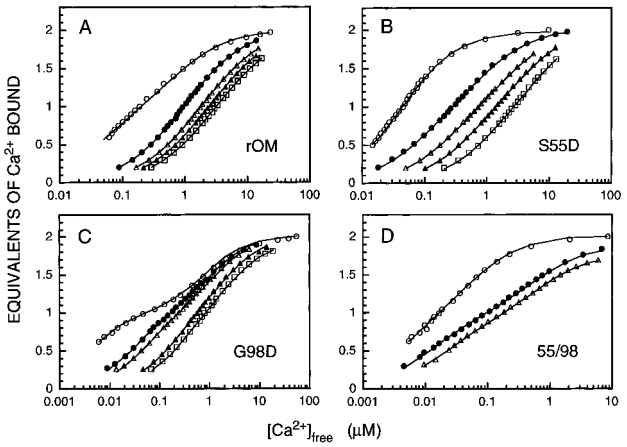

FIGURE 5: Attenuation of Ca^{2+} affinity by Mg^{2+} ion. Samples (100 μM) of the proteins were examined by flow dialysis, either in the absence or in the presence of competing Mg^{2+}. (A) rOM plus 0 mM (○), 2.0 mM (●), 5.0 mM (△), 7.5 mM (▲), and 10 mM (□) Mg^{2+}. (B) G98D plus 0 mM (○), 0.4 mM (●), 1.0 mM (△), 5.0 mM (▲), and 10 mM (□) Mg^{2+}. (C) S55D plus 0 mM (○), 1.0 mM (●), 2.0 mM (△), 3.0 mM (▲), or 4.0 mM (□) Mg^{2+}. (D) 55/98 plus 0 mM (○), 0.4 mM (●), and 1.0 mM (△) Mg^{2+}.

the dissociation constant that they determined for the CD site exceeded 20 mM. They also obtained flow calorimetry data consistent with the occupation of a single site.

The cause of this discrepancy is unknown. However, the rOM preparations isolated in this laboratory reproducibly display behavior consistent with the presence of two Mg^{2+}-binding sites per molecule. $^{45}Ca^{2+}$ flow dialysis experiments were conducted at several fixed levels of Mg^{2+}. Data gathered at 2.0 mM (●), 5.0 mM (△), 7.5 mM (▲), and 10 mM (□) are displayed in Figure 5A. Mg^{2+} dissociation constants were extracted from these data using eqs 8−11, as described in Materials and Methods. The best least-squares fit to each experiment is indicated by the solid line through the points. The Mg^{2+} dissociation constants extracted from these experiments, as well as several others, are listed in Table 3. The average values for the EF and CD sites are 260 ± 100 μM and 1.5 ± 0.2 mM, respectively.

The competitive flow dialysis data were also treated as the sum of two hyperbolas, to extract apparent Ca^{2+} dissociation constants for the two binding sites. These apparent K_{Ca} values were then plotted as a function of Mg^{2+} concentration (Figure 4A). The corresponding Mg^{2+} dissociation constants were calculated from the slopes of the two lines, which equal K_{Ca}/K_{Mg}. The best linear least-squares fit to the line yields Mg^{2+} dissociation constants for the EF and CD sites of 0.29 and 1.6 mM, respectively, consistent with the values extracted by the nonlinear least squares treatment of the individual experiments.

Equilibrium dialysis provides corroborative evidence for binding of Mg^{2+} to both sites. Representative data are shown in the inset to Figure 4A. The solid line through the data represents the fit obtained with apparent dissociation constants of 0.31 and 2.3 mM. Recognizing that there are experimental difficulties attendant to the direct measurement of a dissociation constant exceeding 1 mM, we found that these data nevertheless imply that the K_{Mg} for the weaker site is closer to 1 than 10 mM.

G98D. Replacement of Gly-98 by aspartate, to produce G98D, substantially increases the affinity of one of the two sites for Ca^{2+}. Representative binding data for G98D are

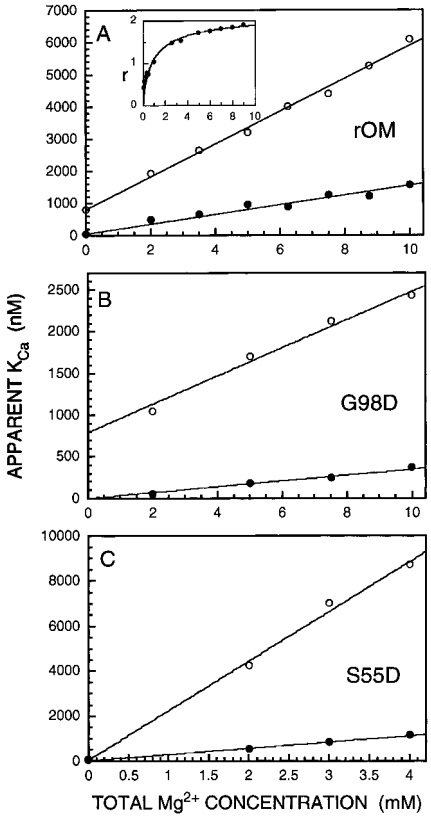

FIGURE 6: Determination of Mg^{2+} binding affinities. $^{45}Ca^{2+}$ flow dialysis was conducted, as described in the text, at fixed levels of Mg^{2+}. Data were treated with an independent two-site model, extracting apparent Ca^{2+} dissociation constants (K_{Ca}'). The K_{Ca}' values thus obtained are plotted vs the Mg^{2+} concentration for rOM (panel A), G98D (panel B), and S55D (panel C). Circles (○) represent data for the CD site; filled circles (●) represent data for the EF site. The solid line through each data set represents the best linear least-squares fit to the data. The inset to panel A presents Mg^{2+} equilibrium dialysis data for wild-type rOM.

presented in Figure 3 (●). If we average the values of k_1 and k_2 from four experiments, we obtain values of 4 ± 3 and 800 ± 40 nM, respectively.

As mentioned above, the dissociation constants for the EF and CD sites in wt rOM are 45 ± 5 and 800 ± 30 nM, respectively. Since the G98D mutation should exert its primary impact on the binding affinity of the EF site, k_1 should correspond to the EF site, while k_2 should correspond to the CD site. These assignments have been confirmed by ^1H NMR spectroscopy. For the purposes of this paper, we will restrict our attention to the methyl signals from Val-106, located in the F helix. These resonances are shifted upfield upon occupation of the EF site, becoming the highest field signals observed in the ^1H spectrum. This behavior, first noted by Parello *et al.* (1974) for carp PV, has also been described for OM (Williams *et al.*, 1987). Presumably, the rearrangement of the F helix that accompanies the binding event brings the Val-106 methyl groups into proximity with the face of the Phe-102 side chain, resulting in a large ring-current shift. The important point here is that the chemical shift of Val-106 is not substantially altered by occupation of the CD site. This is apparent from analysis of site-specific variants, e.g., D94S (data not shown), in which the affinity of the EF site has been weakened to the point that it is no longer occupied first during titrations with Ca^{2+}.

The appearance of the high-field methyl signal at −0.16 ppm from Val-106 is displayed in Figure 5A at various points

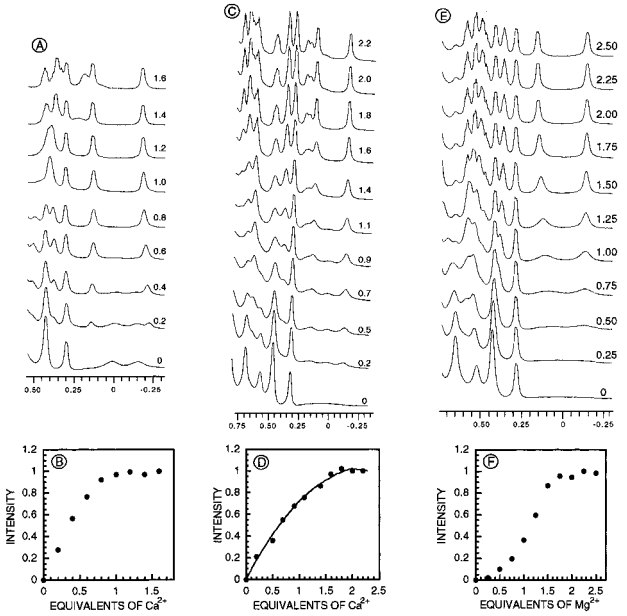

FIGURE 7: Order of occupancy of variant metal ion-binding sites deduced by ^1H NMR. Samples of G98D or S55D were titrated with Ca^{2+} or Mg^{2+}, acquiring the ^1H spectrum after each addition. Samples were prepared in 90% H_2O−10% D_2O and contained 0.15 M NaCl. The pH was 7.4. Spectra are displayed at various points during the titration in panels A, C, and E. The numbers at the right indicate the molar equivalents of metal ion added. The integrated intensity of the signal at $\delta = -0.16$ is plotted as a function of metal ion added in panels B, D, and F. (A and B) Titration of 3.0 mM G98D with Ca^{2+}. (C and D) Titration of 2.6 mM S55D with Ca^{2+}; the solid line through the data points in panel D represents the simulated intensity, assuming that $K_{Ca,EF}$ = 26 nM and $K_{Ca,CD}$ = 67 nM. (E and F) Titration of 3.0 mM S55D with Mg^{2+}.

Table 3: Summary of Mg^{2+}-Binding Studies

		K_{Mg} (μM)	
protein	$[Mg^{2+}]$ (mM)	EF site	CD site
rOM	1.0	157 ± 5	1630 ± 130
	2.0	188 ± 4	1410 ± 45
	3.5	251 ± 6	1510 ± 50
	5.0	253 ± 3	1330 ± 17
	6.25	326 ± 6	1570 ± 30
	7.5	278 ± 4	1570 ± 25
	8.75	330 ± 5	1580 ± 95
	10	291 ± 4	1460 ± 60
	average	260 ± 100	1510 ± 180
G98D	1.0	148 ± 3	3780 ± 250
	2.0	162 ± 4	3540 ± 160
	5.0	115 ± 2	3520 ± 100
	7.5	121 ± 2	3560 ± 60
	10	111 ± 3	4080 ± 170
	average	130 ± 32	3700 ± 400
S55D	0.40	91.4 ± 0.8	31.7 ± 1.0
	1.0	86.5 ± 0.9	30.8 ± 2.4
	2.0	95.9 ± 0.6	25.9 ± 0.8
	3.0	86.2 ± 0.8	29.1 ± 2.1
	4.0	103 ± 3	29.3 ± 1.2
	average	93 ± 10	29 ± 4
55/98	0.40	162 ± 6	34.2 ± 0.6
	1.0	181 ± 11	31.2 ± 1.5
	1.0	153 ± 4.4	28.8 ± 0.6
	average	165 ± 12	31 ± 3

during a titration of G98D with Ca^{2+}. Notice that the increase in intensity is essentially complete with the addition of 1.0 molar equiv (Figure 5B). This result indicates that the EF site of G98D is, in fact, occupied first and that the assignment of the smaller dissociation constant to the EF site is therefore appropriate.

The enthalpy changes that accompany binding of Ca^{2+} to the G98D variant were quite similar to those determined for wild-type rOM. A representative titration is depicted in Figure 4C, and the heat released per addition is plotted as a function of total Ca^{2+} in Figure 4D. Since the four titrations displayed in Figure 4 were conducted at different protein concentrations, the raw data are not directly comparable. However, the integrated heats per addition presented in panels B, D, F, and H have been converted to calories per mole to facilitate comparison among the four proteins. The best fit to an independent two-site model afforded values for ΔH_{EF} and ΔH_{CD} of -4.00 and -3.39 kcal/mol, respectively. Three separate titrations yielded corresponding average values of -4.01 ± 0.03 and -3.42 ± 0.07 kcal/mol. Although the free energy change associated with the binding of Ca^{2+} is roughly 1.4 kcal/mol more exergonic than that associated with binding to the wild-type protein, the enthalpy of binding is essentially unchanged, implying that the increase in affinity has an entropic origin.

Replacement of glycine-98 by aspartate also yields a perceptible increase in the affinity of the EF site for Mg^{2+}. Data from flow dialysis experiments performed at several fixed Mg^{2+} concentrations are displayed in Figure 5B. The Mg^{2+} dissociation constants extracted by nonlinear least-squares analyses of these data sets are listed in Table 3. The average values are 130 ± 30 μM and 3.7 ± 0.4 mM. Alternatively, we can treat the Ca^{2+}-binding data obtained in the presence of Mg^{2+} as the sum of two hyperbolas, as discussed above for rOM, and extract apparent Ca^{2+} dissociation constants. These are plotted vs $[Mg^{2+}]$ in Figure 4B for the CD (○) and EF (●) sites. From the slopes of the two lines, equal to K_{Ca}/K_{Mg}, we extract values for $K_{Mg,EF}$ and $K_{Mg,CD}$ of 125 μM and 4.1 mM. Our assumption that these values corresponded to the EF and CD sites, respectively, was subsequently confirmed by NMR titrations (data not shown). These analyses suggest that the G98D mutation affords a modest increase in the Mg^{2+} affinity for the EF site, by perhaps a factor of 2, and further attenuates the Mg^{2+} affinity of the CD site by a similar factor. The perturbation of the CD site affinity is evidence that the binding events at the two sites in oncomodulin are not completely independent.

S55D. The results of Ca^{2+}-binding measurements on S55D are presented in Figure 3 (◇). The solid line through the data represents the best least-squares fit to an independent two-site model. Averaging the values from three separate experiments, we extracted values for k_1 and k_2 of 26 ± 5 and 67 ± 12 nM, respectively. The corresponding Gibbs free energy changes for binding are $\Delta G_1^\circ = -10.3$ kcal/mol and $\Delta G_2' = -9.7$ kcal/mol. Although it is not possible to assign the binding constants to the CD and EF sites by simple inspection, it is nevertheless apparent that the S55D mutation has greatly increased the affinity of the oncomodulin CD site for Ca^{2+}.

The order of occupancy of the sites was determined by NMR spectroscopy, once again utilizing the Val-106 methyl signals as an indicator for binding at the EF site. The appearance of the high-field region of the spectrum during the course of a titration with Ca^{2+} is depicted in Figure 5C. The signal of interest ($\delta = -0.16$ ppm) was integrated at each point in the titration and plotted vs the molar equivalents of Ca^{2+} added (Figure 5D). The solid line through the data was generated by assuming that the 26 nM dissociation constant corresponded to the EF site and that the 67 nM value corresponded to the CD site. The agreement between the observed and simulated data sets is consistent with the EF site having the higher affinity. The minor increase in affinity at the EF site resulting from the S55D mutation is further indication that the occupation of the two sites in oncomodulin is not strictly independent.

Representative heat effects that accompany binding of Ca^{2+} to S55D are shown in Figure 4E, and the integrated heats per addition are displayed as a function of the total Ca^{2+} concentration in Figure 4F. The best fit to an independent two-site model, assuming $K_{EF} = 26$ nM and $K_{CD} = 67$ nM, is indicated by the solid line through the data. This particular experiment yielded estimates for $\Delta H_{Ca,EF}$ and $\Delta H_{Ca,CD}$ of -6.73 and -2.36 kcal/mol, respectively. The corresponding average values, from three separate titrations, are -6.73 ± 0.03 and -2.45 ± 0.15 kcal/mol. In contrast to the G98D variant, the S55D mutation causes the overall enthalpy change for Ca^{2+} binding to become significantly more exothermic (cf. Figure 4B,F). Moreover, the increased exothermicity is associated with the initial binding event, at the EF site. This result suggests that the S55D mutation, within the CD binding loop, has a significant impact on the metal ion-binding properties of the remote site.

As described above for the wild-type protein and G98D, Mg^{2+} dissociation constants were extracted from $^{45}Ca^{2+}$ flow dialysis experiments conducted at fixed levels of Mg^{2+} (Figure 5C). The average Mg^{2+} dissociation constants extracted from these studies (Table 3) using the model described by eqs 3−5 are 29 ± 4 and 93 ± 10 μM. We have also treated the data gathered at higher Mg^{2+} concentrations with a simple two-site model and extracted apparent Ca^{2+} dissociation constants. These have been plotted as a function of $[Mg^{2+}]$ in Figure 4C, together with the best least-squares fit to the lines. From the slopes of the lines, equal to K_{Ca}/K_{Mg}, we obtained Mg^{2+} dissociation constants of 30 and 91 μM, in agreement with the values obtained from the alternative data analysis.

We assumed that the S55D mutation would exert greater influence on the CD site and tentatively assigned the 29 μM value to the CD site. In fact, when the Mg^{2+}-binding data are subjected to least-squares analysis, the best fit pairs the 29 μM Mg^{2+} dissociation constant with the site having the higher (i.e., 67 nM) Ca^{2+} dissociation constant. We have independently confirmed this assignment by monitoring a Mg^{2+} titration by ^{1}H NMR. The high-field shift of the Val-106 methyl resonance (at -0.16 ppm) once again served as an indicator for occupation of the EF site. The appearance at several points in the titration is displayed in Figure 5E, and the integrated intensities are shown plotted vs equivalents of Mg^{2+} added in Figure 5F. The finding that there is no perceptible occupation of the EF site during the very early stages of the titration implies that the CD site of S55D is in fact occupied first and thus has the higher affinity for Mg^{2+}. The decrease in the magnitude of the Mg^{2+} dissociation constant for the CD site from 1.5 mM to 29 μM affinity resulting from the S55D mutation corresponds to a free energy change ($\Delta\Delta G_{Mg,CD}$) of -2.4 kcal/mol.

55/98. Ca^{2+}-binding data for the 55/98 double variant are presented Figure 3 (◆). The best least-squares fit to the data, indicated by a solid line, yields these values for the dissociation constants: $k_1 = 4 \pm 2$ and $k_2 = 45 \pm 15$ nM. The corresponding values of $\Delta G_1^{\circ\prime}$ and $\Delta G_2^{\circ\prime}$ are -11.4 and -10.0 kcal/mol, respectively. Since the S55D and G98D

mutations occur in the CD and EF sites, respectively, it is not unreasonable that they would have an impact in the double variant comparable to that observed for the single-site variants. Accordingly, we assign k_1, the smaller of the two dissociation constants in 55/98, to the EF site and assign k_2 to the CD site. These assignments have been verified by NMR spectroscopy, as described for the other two variants (data not shown).

The heat pulses that accompany titration of 55/98 with Ca^{2+} are displayed in Figure 4G, and the heat evolved per addition is plotted vs total Ca^{2+} concentration in Figure 4H. The best fit to an independent two-site model, assuming Ca^{2+} dissociation constants of 4 and 45 nM, is indicated by the solid line. The average enthalpy values extracted for the EF and CD sites from three separate determinations were -6.76 ± 0.23 and -3.87 ± 0.33 kcal/mol, respectively. As observed for the S55D variant, the enthalpy change for the EF site is substantially heightened in the 55/98 variant, relative to that of the wild-type protein (cf. Figure 4A,H).

Mg^{2+} dissociation constants were determined for 55/98 by competitive $^{45}Ca^{2+}$ flow dialysis, as described for the other three proteins. Representative data are displayed in Figure 5D. The dissociation constants that we extract for the 55/98 variant are 31 ± 3 and 165 ± 12 μM. These values correspond to the dissociation constants for the CD and EF sites, respectively, as determined by NMR titration (data not shown).

Tb^{3+} Affinity of the S55D, G98D, and 55/98 Variants. Terbium ion has proven to be a useful probe of Ca^{2+}-binding proteins (Horrocks & Sudnick, 1981; Martin, 1983; Evans, 1990). The aquo ion is just weakly luminescent, a consequence of its minuscule extinction coefficient ($\epsilon < 10$) and effective quenching by solvent. Since chelation of the ion reduces its exposure to solvent, binding is generally accompanied by a perceptible increase in the Tb^{3+} quantum yield. Binding can also afford a more efficient path for excitation. The protein-bound Tb^{3+} exhibits a charge-transfer band that overlaps significantly with the protein emission spectrum. Thus, if the binding site is proximal to one or more aromatic residues, there are opportunities for resonance energy transfer.

Oncomodulin contains 10 phenylalanine and two tyrosine residues. However, the data of Hogue *et al.* (1992) indicate (1) that Tyr-57 is responsible for 95% of the energy transfer to the two bound ions in oncomodulin and (2) that occupation of the two binding sites occurs sequentially, with the EF site being occupied first. Although the ions bound at the CD and EF sites are approximately equidistant from Tyr-57, the ion bound at the CD site displays substantially greater luminescent enhancement. Consequently, the early portion of the titration curve (corresponding to nearly exclusive filling of the EF site) exhibits a significantly shallower slope than the remainder [Figure 8A and Hogue *et al.* (1992)]. The titration curve obtained with G98D (Figure 8B) is qualitatively similar to that observed with the wild-type protein, suggesting that, as in the wild-type protein, the CD site is occupied only after the EF site has been filled.

Interestingly, whereas the EF site of S55D has the higher affinity for Ca^{2+}, the CD site exhibits the higher affinity for Tb^{3+}. Observe that, for S55D, the luminescence at 545 nm increases sharply with the first addition of Tb^{3+} and is largely complete (>80%) with the addition of 1 molar equiv (Figure 8C, ●). This result indicates that the CD site of S55D has the higher affinity for Tb^{3+} ion and thus tends to be occupied first. Similar behavior has been observed by Wang *et al.* (1982, 1984) with calmodulin; i.e., the binding sites in the N-terminal EF domain exhibit higher affinity for the lanthanide despite their lower affinity for Ca^{2+}. It is worth emphasizing that, if the S55D titration is performed with direct excitation of the ion (Figure 8C, ○), the luminescence intensity levels off with the addition of 2 molar equiv, evidence that the S55D variant retains two functional Tb^{3+} binding sites.

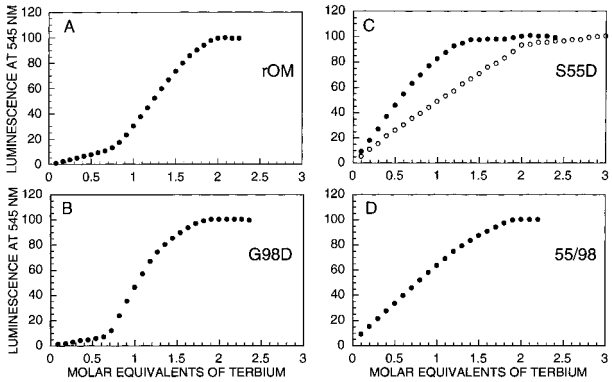

FIGURE 8: Tb^{3+} luminescence studies on rOM, S55D, G98D, and 55/98. Samples (20 μM) of the proteins were titrated with Tb^{3+} ion in fluorescence cuvettes having a 10 mm path length, and the intensity of the Tb^{3+} luminescence at 545 nm was measured after each addition. λ_{ex} was either 280 nm (●) for indirect excitation or 360 nm (○) for direct excitation. The nominal band-pass was 2 nm for both excitation and emission.

In the case of the 55/98 variant, the luminescence at 545 nm increases almost linearly up to the addition of 2 molar equiv of Tb^{3+} (Figure 8D). This result suggests that the CD and EF sites in this variant have comparable affinities for the ion.

DISCUSSION

The coordination chemistry of spherical ions like Ca^{2+} or Mg^{2+} is dominated by electrostatic effects. The equilibrium binding affinity observed for an EF-hand site reflects the difference between the free energy of dehydration (dependent on ionic charge and radius) and the free energy of interaction with the ligand array. As Falke has observed (Falke *et al.*, 1994), the latter can be tuned by several mechanisms: the number of ligands (i.e., coordination number), the size of the binding pocket (cavity size), and charge selectivity (arising from electrostatic repulsion between the coordinating oxygens). Notice, however, that these variables are not strictly independent. For example, cavity size is governed in part by electrostatic repulsion between the ligands. And the observed coordination number, seven for Ca^{2+} and six for Mg^{2+}, may represent a compromise between cavity size and interligand repulsion. Given the interdependence of these factors, it is not surprising that a quantitative description of electrostatic effects in these systems remains out of reach.

Forsén and his colleagues have addressed the significance of electrostatic contributions in the calbindin D_{9k} system, preparing a series of charge-deletion variants at noncoordinating residues in the N-terminal Ca^{2+}-binding site, a pseudo-EF hand (Wendt *et al.*, 1988; Martin *et al.*, 1990; Akke & Forsén, 1990). The E17Q, D19N, and E26Q mutations were examined alone and in combination, with the objective of defining the role of protein surface charges on Ca^{2+} affinity

and the kinetics of Ca^{2+} binding. These investigators found that, at physiologically relevant ionic strengths (0.1 M KCl), elimination of a single negative charge reduced the equilibrium binding affinity by 0.3−0.4 kcal/mol. The combined mutations reduced affinity by 2.4 kcal/mol. The lower affinity was attributed to a substantial reduction in the rate of association, since the rate of dissociation was essentially unchanged in the variant proteins. The authors speculated that the initial encounter complex formed between the protein and metal is strengthened by electrostatic interactions between postively charged metal ion and the negative side chains. Thus, the surface charge distribution provides a mechanism for tuning the association kinetics and equilibrium binding affinity.

However, electrostatic effects can also influence ion-binding properties indirectly, through perturbations of macromolecular structure, either locally or globally. The impact on the immediate coordination environment is embodied in the acid-pair hypothesis (Reid & Hodges, 1980). Although anionic ligands increase the attraction for Ca^{2+}, the resulting localization of negative charge in the binding pocket can cause electrostatic destabilization. As a consequence of these opposing factors, Reid and Hodges proposed that Ca^{2+} affinity should be maximized in an EF hand having four anionic ligands paired on the $+x,-x$ and $+z,-z$ axes.

Against this theoretical backdrop, the ion-binding properties of the S55D and G98D variants of oncomodulin appear somewhat anomalous. Rather than decreasing the binding affinity, each substantially increases the Ca^{2+}-binding affinity of its host binding site. Replacement of serine-55 by aspartate reduces $K_{Ca,CD}$ from 800 to 67 nM, a 1.4 kcal/mol improvement in the $\Delta G°'$ for Ca^{2+} binding. Similarly, replacement of glycine-98 by aspartate reduces $K_{Ca,EF}$ from 45 to 4 nM, likewise corresponding to a 1.4 kcal/mol reduction in the free energy of Ca^{2+}-binding.

Oncomodulin is noteworthy for its uncharacteristically low affinity for Ca^{2+} and Mg^{2+}. Assuming average K_{Ca} and K_{Mg} values of 10 nM and 50 μM for a typical PV isoform, the $\Delta G_{Ca}°'$ and $\Delta G_{Mg}°'$ values measured for oncomodulin are approximately 3.5 and 2.9 kcal/mol less favorable than expected. We have invested considerable effort in the identification of factors responsible for this attenuation of binding affinity (Hapak *et al.*, 1989; Palmisano *et al.*, 1990; Treviño *et al.*, 1991). Interestingly, we find that the combined S55D and G98D mutations restore 3.2 kcal/mol of favorable Ca^{2+}-binding energy and 2.5 kcal/mol of favorable Mg^{2+}-binding energy. Thus, it is possible that the attenuation of ion-binding affinity in oncomodulin has a substantial electrostatic component.

The DSC data may offer some insight into the origin of the increased affinity of these variants for Ca^{2+}. Wild-type apo-rOM denatures at 51.8 °C, with $\Delta H_{cal} = 66$ kcal/mol. Using eq 12, we estimate a conformational free energy at 25 °C of 3.9 kcal/mol. The S55D and G98D mutations both destabilize the apo state of the protein, relative to the state of the wild-type protein, reducing T_d to 48.9 and 51.1 °C, respectively. Combination of the two mutations, to produce 55/98, further lowers T_d to 47.9 °C. The enthalpies of denaturation are likewise reduced in S55D, G98D, and 55/98 to 51, 58, and 49 kcal/mol, respectively. The calculated stabilities at 25 °C for the three proteins are 2.6, 3.2, and 2.4 kcal/mol, and the corresponding alterations in stability resulting from the mutations ($\Delta\Delta G_{conf}$) are −1.3, −0.7, and −1.5 kcal/mol. Consistent with the effect that we see in oncomodulin, Akke and Forsén (1990) observed that the neutralization of surface anionic charges on calbindin D_{9k} caused a significant increase in conformational stability.

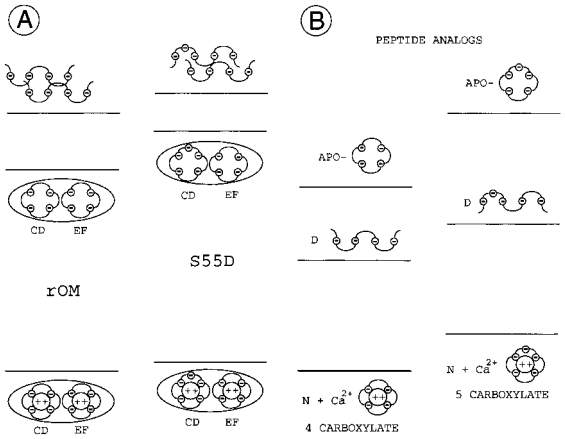

FIGURE 9: Alterations in conformational stability caused by the S55D and G98D mutations. (A) Qualitative changes in free energy, inferred from the DSC analyses, that accompany the S55D mutation. Relative placement of the energy levels is intended to emphasize the differential impact of the additional negative charge on the Ca^{2+}-bound, apo-, and denatured forms of the proteins. (B) Corresponding energy level diagram for a model peptide system. The primary intent here was to emphasize the qualitatively different nature of the peptide and intact protein systems, i.e., the inversion of the apo- and denatured (D) energy levels.

The reductions in ΔT_d and ΔH_{cal} that accompany the S55D, G98D, and 55/98 mutations suggest that the apo forms of the variants are less tightly folded than the wild-type protein. The increased exothermicity of Ca^{2+} binding observed for the S55D and 55/98 variants is consistent with this idea. The heat released upon Ca^{2+} binding to rOM and the variant proteins presumably reflects the conformational reorganization of the polypeptide and concomitant establishment of numerous van der Waals contacts. If we assume, for example, that apo-S55D is less tightly folded than apo-rOM, then when the protein binds Ca^{2+}, and adopts a compact state comparable to that of Ca^{2+}-bound rOM, a relatively larger number of noncovalent interactions would be established. This difference would be manifested in the more exothermic heat of Ca^{2+} binding.

In contrast to the apo-proteins, the Ca^{2+}-bound variants denature at higher temperatures than rOM. Whereas the wild-type protein denatures at 92.8 °C, melting temperatures of 95.1, 95.3, and 97.4 °C are observed for S55D, G98D, and 55/98, respectively. The estimated conformational stability for rOM is 12.6 kcal/mol. The corresponding values for S55D, G98D, and 55/98 are 13.1, 15.0, and 15.9 kcal/mol. Thus, the mutations increase the conformational stability of the variants by +0.5, +2.4, and +3.3 kcal/mol.

The CD and EF binding loops of wild-type oncomodulin harbor six and five carboxylates, respectively. Due to increased electrostatic repulsion, introduction of an additional carboxylate into either site should destabilize, to differing degrees, the denatured, apo, and Ca^{2+}-bound states (Figure 9A). The apo form should be perturbed to the greatest extent, since the native fold forces the carboxylates into proximity, without benefit of the stabilizing presence of Ca^{2+}. In the denatured state, the carboxylates can maximize their separation, within the limits imposed by their position in the sequence. And in the Ca^{2+}-bound form, the electrostatic

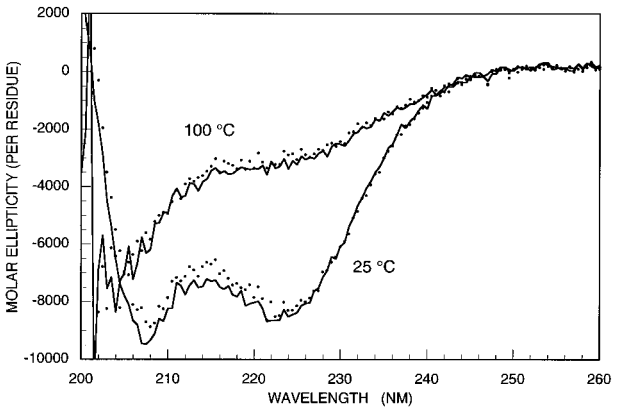

FIGURE 10: CD spectra of native and denatured rOM in the presence and absence of Ca^{2+}. The CD spectrum of native apo-rOM (●) was acquired at 25 °C in an AVIV 62DS circular dichroism spectrometer equipped with a thermostatted cell holder. The temperature was then raised to 100 °C, and the spectrum was reacquired (●). Ca^{2+} was then added to afford a final concentration of 5.0 mM; the sample was allowed to equilibrate for 30 min, and the spectrum was reacquired (100 °C, solid line). Finally, the temperature was returned to 25 °C, and the spectrum of the native Ca^{2+}-bound protein was obtained (25 °C, solid line). The sample, in a 0.1 cm path length cell, contained 0.2 mg/mL rOM, in 0.15 M NaCl (pH 7.4). The appearance of the CD spectrum is highly reminiscent of data seen with other parvalbumin isoforms [e.g., Closset and Gerday (1975)].

repulsion is partially neutralized by the divalent cation. The differential destabilization of the apo and denatured states shrinks the energetic gap between the two states, thereby lowering T_d. At the same time, preferential destabilization of the apo state widens the gap between the apo and Ca^{2+}-bound states, which corresponds to the free energy of Ca^{2+} binding. Thus, differential destabilization of the apo and Ca^{2+}-bound forms may contribute to the observed increase in Ca^{2+} affinity.

Presumably, this mechanism is not applicable to the model peptide systems, since the latter have little or no intrinsic conformational stability in the absence of Ca^{2+}. As indicated in Figure 9B, the correctly folded apo-peptide lies at a higher energy than the random coil form. This fundamental difference in the conformational energetics of the intact proteins and the peptide analogs may help explain why the acid-pair hypothesis is of substantial predictive value for peptides but can fail for the intact proteins.

Implicit in this argument is the assumption that the unfolded states resulting from thermal denaturation are equivalent, or nearly so, in the presence and absence of Ca^{2+}. Note that the addition of 5.0 mM Ca^{2+} to the thermally denatured form of wild-type oncomodulin causes no detectable alteration in the far-UV CD spectrum (Figure 10). This result implies that the presence of Ca^{2+} does not cause retention of residual secondary structure in the denatured form. Consequently, any Ca^{2+}−peptide interactions that occur in the denatured state must stem from the very weak association between Ca^{2+} and isolated carboxylate groups. Estimates for the dissociation constant of the Ca^{2+}−acetate complex range from 1.6 to 1.8 M at roughly physiological ionic strengths (Cannan & Kibrick, 1938; Joseph, 1946). In this light, the assumption that the denatured states are approximately equivalent appears reasonable.

Although the S55D and G98D mutations afford comparable increases in Ca^{2+}-binding affinity, they also provide several interesting contrasts. Substitution of aspartate for S55 reduces K_{Mg} for the host CD site from 1.5 mM to 30 μM, a 50-fold increase in affinity, and substantially reduces K_{Mg} at the remote EF site as well, from 260 to 90 μM. The heightened affinity for Mg^{2+} is reflected in the markedly increased thermal stability of S55D. Whereas rOM denatures at 68.5 °C in NaCl/Hepes buffer containing 20 mM Mg^{2+}, the apparent T_d for S55D is 79.0 °C. By contrast, replacement of Gly-98 by aspartate has a fairly modest impact on the host EF site, reducing K_{Mg} from 260 μM in rOM to 130 μM, and actually weakens binding at the remote CD site, raising K_{Mg} for the CD site from 1.5 to 3.7 mM ($\Delta\Delta G_{Mg} = +0.6$ kcal/mol).

Significantly, the increase in Ca^{2+}-binding affinity resulting from G98D appears to have an entropic origin. G98D causes very little perturbation of the binding enthalpy, but the overall $-T\Delta S$ term increases in magnitude from −10.8 to −12.3 kcal/mol. In wild-type rOM, a water molecule serves as the $-x$ ligand. The more favorable entropic contribution to Ca^{2+} binding by G98D would be consistent with replacement of the coordinating water molecule by the aspartate carboxylate. However, the crystallographic data for EF-hand motifs in calmodulin, troponin C, and various parvalbumins suggest that the distance between the C_α of the $-x$ residue and the bound Ca^{2+} is too large to be spanned by an aspartyl side chain [e.g., McPhalen *et al.* (1991)].

Thus, it is likely that the more favorable entropy of Ca^{2+} binding observed for G98D has a conformational origin. In the wild-type protein, with a glycyl residue at position 98, the binding loop enjoys substantial conformational flexibility in the apo form of the protein. The decrease in mobility attendant to coordination of Ca^{2+} would be entropically unfavorable. By contrast, the flexibility of the EF loop in apo-G98D should be significantly reduced, since the side chain of Asp-98 would restrict mobility. As a consequence, the EF site of the G98D variant would presumably experience a relatively smaller loss of conformational entropy upon Ca^{2+} binding.

In contrast to G98D, the increased affinity for Ca^{2+} displayed by S55D apparently results from a more favorable enthalpy of binding (the overall ΔH for Ca^{2+} binding goes from −7.5 to −9.1 kcal/mol).

The contrasts between S55D and G98D emphasize the importance of mutational context. The CD binding site is located in the middle of the PV sequence so that conformational adjustments in the binding loop may require energetically expensive alterations in the flanking regions of the polypeptide. Thus, substitutions at residue 55 may significantly perturb the global polypeptide fold. By contrast, the EF site is positioned close to the C-terminal end of the molecule. As a consequence, conformational rearrangements in the vicinity of residue 98 can be more local and need not involve the rest of the molecule. One might imagine that the increased repulsion attendant to replacement of glycine-98 with aspartate could be largely offset by partial unfolding of the EF loop and F helix. The fact that the reduction of stability observed for apo-G98D ($\Delta T_d = -0.7$) is significantly smaller than that observed for apo-S55D ($\Delta T_d = -2.9$) suggests that the conformational alteration is more restricted.

The binding and calorimetry data presented above contain several indications of cooperative interactions between the binding sites. The results of Ca^{2+}-binding studies on additional site-specific variants of oncomodulin suggest that Ca^{2+} binding occurs with negative cooperativity in wild-

type oncomodulin (R. C. Hapak and M. T. Henzl, unpublished observations). For example, the D94S mutation, which weakens binding at the EF site to the point that it is no longer preferentially occupied, increases the Ca^{2+} affinity of the CD site. This finding implies that the conformation of the protein resulting from the Ca^{2+}-binding event at the EF site is not the preferred one for binding at the CD site.

This antagonism could explain the impact of the G98D mutation on the ion-binding properties of the CD site. Since the Mg^{2+} dissociation constants for the CD and EF sites differ by just a factor of 5 in wild-type rOM, occupation of the two sites is not strictly ordered. The increase in Mg^{2+} affinity at the EF site attendant to the G98D mutation would cause the binding to become more ordered. Consequently, the Mg^{2+} ion bound at the CD site would be increasingly forced to bind to the unfavorable conformation dictated by the EF binding event, leading to the further attenuation of CD site affinity. By contrast, the binding of Ca^{2+} to the wild-type protein is already highly ordered, a consequence of the 20-fold difference in the Ca^{2+} dissociation constants of the CD and EF sites. Thus, the increased Ca^{2+} affinity of the EF site resulting from the G98D mutation has no perceptible effect on the Ca^{2+} affinity at the remote site.

Of course, any negatively cooperative effects should be reciprocal. Thus, in the absence of other considerations, the increase in Ca^{2+} and Mg^{2+} affinity at the CD site resulting from the S55D mutation should antagonize binding at the EF site. In fact, the S55D mutation affords perceptible increases in both the Ca^{2+} and Mg^{2+} affinities of the EF site. Conceivably, the substitution of aspartate, with its longer side chain, for serine at the $+z$ postion reduces the conformational rearrangement of the binding loop that accompanies binding at the CD site, thereby reducing the impact of the CD binding event at the EF site. Clarification of the cooperative interactions between the CD and EF sites in oncomodulin remains a challenging issue for future investigations.

It is apparent from these studies that introduction of a fifth carboxylate into the coordination sphere of an EF-hand motif does not necessarily reduce the affinity of that site for Ca^{2+}. The critical factor is not necessarily the repulsion generated in the bound complex, but rather the difference in electrostatic repulsion between the apo and bound forms. At this point, we do not know how general this phenomenon is. It would be interesting to examine the consequences of comparable mutations in other EF hand proteins. For example, site 2 of skeletal troponin C has a ligand array identical to that of the oncomodulin CD site (Collins *et al.*, 1977). Would replacement of the $+z$ serine by aspartate yield an increase in Ca^{2+}- and Mg^{2+}-binding affinity comparable to that observed for the S55D mutation in oncomodulin? Similarly, site I of calmodulin has a ligand array reminiscent of the EF site of oncomodulin, but with threonine at the $-x$ position instead of glycine (Watterson *et al.*, 1980). Would replacement of the $-x$ threonine by aspartate raise the affinity of that site for Ca^{2+}? In this context, it is worth emphasizing that the oncomodulin CD site is unusual for a parvalbumin, having an aspartate at the *-x* coordination position instead of the consensus glutamate. Hence, it would be interesting to see whether the S55D mutation has a similar effect in a more typical parvalbumin CD site, in which the $-x$ ligand is supplied by a glutamyl carboxlate. Related to this issue, does the G98E mutation have an impact on the EF site comparable to G98D? Experiments to address this issue on representative α- and β-PV isoforms are currently in progress.

REFERENCES

Ahmed, F., Przybylska, M., Rose, D. R., Birnbaum, G. I., Pippy, M. E., & MacManus, J. P. (1990) *J. Mol. Biol. 216*, 127−140.

Ahmed, F., Rose, D. R., Evans, S. V., Pippy, M. E., & To, R. (1993) *J. Mol. Biol. 230*, 1216−1224.

Akke, M., & Forsén, S. (1990) *Proteins 8*, 23−29.

Becktel, W. J., & Schellman, J. A. (1987) *Biopolymers 26*, 1859−1877.

Brandts, J. F., & Lin, L.-N. (1990) *Biochemistry 29*, 6927−6940.

Briggner, L.-E., & Wadsö, I. (1991) *Biochem. Biophys. Methods 22*, 101−118.

Cannan, R. K., & Kibrick, A. (1938) *J. Am. Chem. Soc. 60*, 2314−2320.

Christensen, J. J., Hansen, L. D., & Izatt, R. M. (1976) *Handbook of Proton Ionization Heats and Related Thermodynamic Quantities*, John Wiley & Sons, New York.

Closset, J., & Gerday, C. (1975) *Biochim. Biophys. Acta 405*, 228−235.

Collins, J. H., Greaser, M. L., Potter, J. D., & Horn, M. J. (1977) *J. Biol. Chem. 252*, 6356−6362.

Colowick, S. P., & Womack, F. C. (1968) *J. Biol. Chem. 244*, 774−776.

Cox, J. A., Milos, M., & MacManus, J. P. (1990) *J. Biol. Chem. 265*, 6633−6637.

Evans, C. H. (1990) *Biochemistry of the Lanthanides*, Plenum Press, New York.

Falke, J. J., Drake, S. K., Hazard, A. L., & Peersen, O. B. (1994) *Q. Rev. Biophys. 27*, 219−290.

Filimonov, V. V., Pfeil, W., Tsalkova, T. N., & Privalov, P. L. (1978) *Biophys. Chem. 8*, 117−122.

Freire, E., Mayorga, O. L., & Straume, M. (1990) *Anal. Chem. 62*, 950−959.

Gerday, C. (1988) in *Calcium and Calcium-binding Proteins. Molecular and Functional Aspects* (Gerday, C., Bolis, L., & Gilles, R., Eds.) pp 23−39, Springer-Verlag, Berlin.

Gillen, M. F., Banville, D., Rutledge, R. G., Narang, S., Seligy, V. L., Whitfield, J. F., & MacManus, J. P. (1987) *J. Biol. Chem. 262*, 5308−5312.

Golden, L. F., Corson, D. C., Sykes, B. D., Banville, D., & MacManus, J. P. (1989) *J. Biol. Chem. 264*, 20314−20319.

Haner, M., Henzl, M. T., Raissouni, B., & Birnbaum, E. R. (1984) *Anal. Biochem. 138*, 229−234.

Hapak, R. C., Lammers, P. L., Parmisano, W. A., Birnbaum, E. R., & Henzl, M. T. (1989) *J. Biol. Chem. 264*, 18751−18760.

Heizmann, C. W. (1984) *Experentia 40*, 910−921.

Henzl, M. T., Treviño, C. L., Dvorakova, L., & Boschi, J. M. (1992) *FEBS Lett. 314*, 130−134.

Hogue, C. W. V., MacManus, J. P., Banville, d., & Szabo, A. G. (1992) *J. Biol. Chem. 267*, 13340−13347.

Horrocks, W. D., Jr., & Sudnick, D. R. (1981) *Acc. Chem. Res. 14*, 384−392.

Joseph, N. R. (1946) *J. Biol. Chem. 164*, 529−541.

Kauffman, J. F., Hapak, R. C., & Henzl, M. T. (1995) *Biochemistry 34*, 991−1000.

Kretsinger, R. H. (1980) *CRC Crit. Rev. Biochem. 8*, 119−174.

Kretsinger, R. H. (1987) *Cold Spring Harbor Symp. Quant. Biol. 52*, 499−510.

MacManus, J. P., & Whitfield, J. F. (1983) *Calcium Cell Funct. 4*, 411−440.

Marsden, B. J., Hodges, R. S., & Sykes, B. D. (1988) *Biochemistry 27*, 4198−4206.

Martin, R. B. (1983) in *Calcium in Biology* (Spiro, T. G., Ed.) pp 235−270, John Wiley & Sons, New York.

Martin, S. R., Linse, S., Johansson, C., Bayley, P. M., & Forsén, S. (1990) *Biochemistry 29*, 4188−4193.

McPhalen, C. A., Strynadka, N. C. J., & James, M. N. G. (1991) *Adv. Protein Chem. 42*, 77−144.

Palmisano, W. A., Treviño, C. L., & Henzl, M. T. (1990) *J. Biol. Chem. 265*, 14450−14456.

Parello, J., Cavé, A., Puigdomenech, P., Maury, C., Capony, J. P., & Pechere, J.-F. (1974) *Biochimie 56*, 61−76.
Privalov, P. L. (1979) *Adv. Protein Chem. 33*, 167−241.
Procyshyn, R. M., & Reid, R. E. (1994a) *Arch. Biochem. Biophys. 311*, 425−429.
Procyshyn, R. M., & Reid, R. E. (1994b) *J. Biol. Chem. 269*, 1641−1647.
Reid, R. E. (1987) *Biochemistry 26*, 6071−6073.
Reid, R. E. (1990) *J. Biol. Chem. 265*, 5971−5976.
Reid, R. E., & Hodges, R. S. (1980) *J. Theor. Biol. 84*, 401−444.
Seamon, K. B., & Kretsinger R. H. (1983) in *Calcium in Biology* (Spiro, T. G., Ed.) pp 3−51, John Wiley & Sons, New York.
Straume, M., & Freire, E. (1992) *Anal. Biochem. 203*, 259−268.
Strynadka, N. C. J., & James, M. N. G. (1989) *Annu. Rev. Biochem. 58*, 951−998.
Sturtevant, J. M. (1987) *Annu. Rev. Phys. Chem. 38*, 463−488.
Treviño, C. L., Boschi, J. M., & Henzl, M. T. (1991) *J. Biol. Chem. 266*, 11301−11308.
Wang, C.-L. A., Aquaron, R. R., Leavis, P. C., & Gergely, J. (1982) *Eur. J. Biochem. 124*, 7−12.
Wang, C.-L. A., Leavis, P. C., & Gergely, J. (1984) *Biochemistry 23*, 6410−6415.
Watterson, D. M., Sharief, F., & Vanaman, T. C. (1980) *J. Biol. Chem. 255*, 462−475.
Wendt, B., Hofmann, T., Martin, S. R., Bayley, P., Brodin, P., Grundström, T., Thulin, E., Linse, S., & Forsén, S. (1988) *Eur. J. Biochem. 175*, 439−445.
White, H. D. (1988) *Biochemistry 27*, 3357−3365.
Williams, T. C., Corson, D. C., Sykes, B. D., & MacManus, J. P. (1987) *J. Biol. Chem. 262*, 6248−6256.
Wnuk, W., Cox, J. A., & Stein, E. A. (1982) *Calcium Cell Funct. 2*, 243−278.
Wyman, J., & Gill, S. J. (1990) *Binding and Linkage*, pp 44−46, University Science Books, Mill Valley, CA.

BI952184D